Origin of Low Thermal Conductivity in Nuclear Fuels

Quan Yin and Sergey Y. Savrasov

Department of Physics, University of California, Davis, California 95616, USA

(Received 14 February 2008; published 6 June 2008)

Using a novel many-body approach, we report lattice dynamical properties of UO_2 and PuO_2 and uncover various contributions to their thermal conductivities. Via calculated Grüneisen constants, we show that only longitudinal acoustic modes having large phonon group velocities are efficient heat carriers. Despite the fact that some optical modes also show their velocities which are extremely large, they do not participate in the heat transfer due to their unusual anharmonicity. Ways to improve thermal conductivity in these materials are discussed.

DOI: 10.1103/PhysRevLett.100.225504 PACS numbers: 63.20.−e, 28.41.Bm

Today's nuclear fuels are based on ^{235}U and ^{239}Pu elements where in a typical setup, a nuclear reaction heats up a pellet made of either UO_2 or its mixture with PuO_2 and the heat is transformed to electrical energy. One of the major issues is to conduct the heat from a core of the pellet to its outer area which makes the evaluation of a high temperature thermal conductivity a key problem. Unfortunately, the thermal conductivity of UO_2 is very low, and the search for alternative materials continues.

In the present Letter, we argue that it is the unexpectedly large anharmonicity of optical modes that results in a very low thermal conductivity of modern nuclear fuels. Consider semiconducting UO_2 which is a main element of UOX fuel, or a blend of U and Pu oxides which is a major substance of MOX fuel. The heat from the core of the pellet in these insulating systems is carried by phonons which are known to be very inefficient heat conductors. This brings a whole set of complex problems such as causing fuel pellets to crack and degrade prematurely, necessitating replacement before the fuel has been depleted.

Unfortunately, studying thermal conductivity [1] as well as properties such as crystal structures, phase diagrams, lattice dynamics, and structural instabilities of the actinide based materials is a formidable theoretical problem. Most of the previous works have concentrated on molecular dynamic simulations with empirically adjusted interatomic potentials [2,3]. However, the $5f$ electrons in actinides are close to a localization-delocalization or Mott transition as it has been recently demonstrated for Plutonium metal [4–6]. UO_2 and PuO_2 are Mott-Hubbard insulators with energy gaps at both low and high temperatures. Despite an impressive set of past theoretical studies [7–13], the spectral functions of the high temperature paramagnetic regime cannot be obtained by static mean-field theories such as the Density Functional Theory [14] and require a genuine many-body treatment [15].

In the present Letter, we use a novel electronic structure method [15] capable of describing Mott insulating materials in order to address the structural properties of modern nuclear fuels. Both UO_2 and PuO_2 are calculated using a combination of local density approximation (LDA) [14] and Dynamical Mean-Field Theory (DMFT) [16,17] where relativistic $5f$ shells of Uranium and Plutonium atoms are treated by exact diagonalization of corresponding many-body Hamiltonians obtained by allowing a hybridization between the $5f$-electrons and the nearest oxygen $2p$ orbitals. The method we use for studying phonons and anharmonic effects allows qualitative insights on thermal conductivity with the possibility to screen prospective materials for the nuclear industry.

It is well known that a strong spin-orbit coupling of about 1 eV present in actinides splits 14-fold degenerate f level onto $f_{5/2}$ and $f_{7/2}$ states. Group theoretical considerations assume that under cubic crystal symmetry, the $f_{5/2}$ sixfold degenerate level is further split onto Γ_8 quadruplet and Γ_7 doublet. In both UO_2 and PuO_2, the Γ_8 level comes approximately 0.1 eV below the Γ_7 state, and valence arguments make it occupied by two electrons for the case of UO_2 and fully occupied by four electrons for the case of PuO_2. This sequence of the levels dictates the low temperature properties of these two materials: The UO_2 becomes magnetic where the 9-fold degenerate many-body ground state of the atomic f-shell $^3H_4$ with $J = 4$ is split onto 4 subsets, among which the lowest triplet state of Γ_5 symmetry carries the moment of about $1.7–1.8\mu_B$ below the Néel temperature of 30.8 K [18]. On the other hand, PuO_2 has the filled Γ_8 one-electron level, making its atomic $^3K_4$ multiplet split in such way that the nonmagnetic Γ_1 singlet comes lowest.

The cluster exact diagonalizations which are carried out in our LDA + DMFT calculations support this atomic physics picture and only marginally alter the self-energies for the f-electrons from their corresponding atomic values. In fact, the crystal structures of both materials show that the actinide elements are centered in the cubic environment (see Fig. 1) assuming that only relativistic Γ_7 orbital (its shape is shown in Fig. 1) of the $f_{5/2}$ state is properly coordinated by and strongly hybridized with the O $2p$ states. The corresponding hybridization functions $\Delta_\alpha(\omega)$

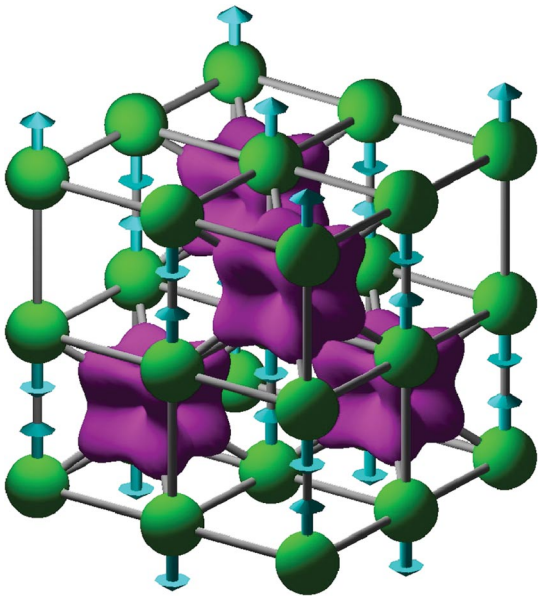

FIG. 1 (color). Crystal structure of UO_2 and PuO_2: Uranium or Plutonium atoms (their shapes are shown by the Γ_7 relativistic orbital densities) are centered inside the cubic lattice made by oxygen atoms. The arrows show the displacements of oxygens associated with the dispersive longitudinal optical mode.

are well fit by the single pole approximation, $\Delta_\alpha(\omega) = |V_\alpha|^2/(\omega - P_\alpha)$, producing only significant values of the matrix elements $V_\alpha \sim 1$ eV for Γ_7 in the $j = 5/2$ manifold and several times smaller values for the Γ_8 orbitals. Similar effect is seen for $\Gamma_6, \Gamma_7, \Gamma_8$ states in the $j = 7/2$ manifold. The position of the dispersive oxygen band centered at the pole P_α comes out -1 to -5 eV below the occupied f states, making both materials classical Mott-Hubbard insulators. It is important to realize that the DMFT aspect is crucial here in order to recover insulating behavior of UO_2 above T_N and of PuO_2 at any T. We find that the fundamental energy gaps produced by the lower (occupied) and upper (unoccupied) Hubbard bands are equal to 2.2 eV for UO_2 and 2.5 eV for PuO_2. The experimental energy gap in UO_2 is of the order of 2 eV [18]. These data are obtained utilizing a recently developed matrix expansion algorithm [19] which helps to perform full self-consistency with respect to both the charge densities as required by the LDA procedure and the $5f$-electron spectral functions as required by the DMFT. Here, the $5f$-electron self-energies extracted from the cluster exact diagonalization are subsequently fit using three-pole interpolation. An effective parameter $U_{\text{eff}} = 3$ eV describing the on-site Coulomb repulsion among the $5f$ electrons is used while the other Slater integrals ($F^{(2)}$, $F^{(4)}$ and $F^{(6)}$) are computed from atomic physics, and are subsequently rescaled to 80% of their values to account for the effect of screening [20].

In order to calculate the phonon spectra of UO_2 and PuO_2, we utilize a new relativistic linear response phonon method which has been recently generalized for the LDA + DMFT scheme [21] and has recently demonstrated its predictive power by finding the phonon spectrum of δ-Pu metal [22] prior to the experiment [23]. In this linear response calculation, the pole interpolation for the self-energies reduces the calculation of the dynamical matrix to standard linear response theory. Since our interest lies in the thermal conductivity at operating temperatures of nuclear fuels, we perform the calculations of the phonon dispersions for paramagnetic phases of the materials with the f-electron self-energies extracted at $T = 1000$ K, where not only the many-body ground states (Γ_5 for UO_2 and Γ_1 for PuO_2) but also various low-lying excited states are beginning to contribute.

Figure 2 shows the comparison between our calculated (filled symbols connected by lines) and measured (open symbols) [24] phonon spectrum for UO_2 along two symmetry lines of the Brillouin Zone. Figure 3 presents our predicted phonon spectrum for PuO_2. Overall, both materials demonstrate very similar dispersions. Because of various numerical inaccuracies and approximate treatment of many-body effects, which, in particular, involves the use of U_{eff}, the overall mismatch between our theory and experiment for UO_2 is about 15%. Part of the discrepancy may be due to the fact that the measurements were done at 300 K, but we do not expect it to be essential. The same 15% accuracy can be assumed for our predicted phonon dispersions in PuO_2. Increasing the U_{eff} to 4–5 eV marginally affects the overall phonon spectra although it makes optical modes 10–20% harder.

Our calculations reveal the following features of lattice dynamics in these materials. First, acoustic modes are located at the low frequency region of the spectrum producing the group velocities of about 700 m/s for transverse acoustic (TA) and 1100 m/s for longitudinal acoustic (LA) modes (see also Table I). There are two groups of transverse and longitudinal optical modes which we sche-

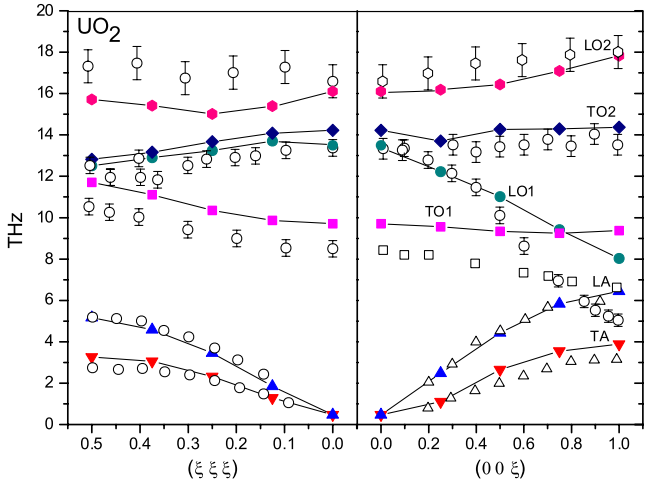

FIG. 2 (color online). Calculated phonon dispersions (filled symbols connected by lines) and experimentally measured phonons (open symbols) [24] for UO_2.

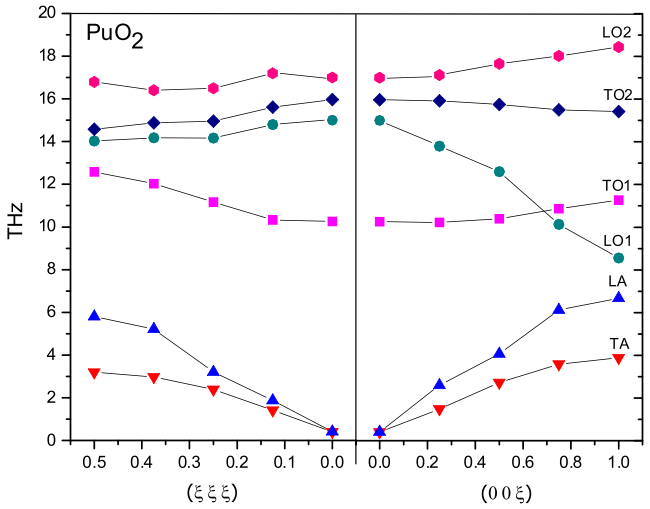

FIG. 3 (color online). Calculated phonon dispersions (filled symbols connected by lines) for PuO_2. No experiment available.

matically label as TO1, LO1 and TO2, LO2. The first group represents lattice vibrations associated with the out-of-phase displacements of oxygens and little involvement of U or Pu atoms. The second group represents the lattice vibrations of oxygens which vibrate in-phase against U or Pu atoms.

There is a remarkably dispersive mode LO1 which has a very large group velocity along (001) direction in both materials. This mode is primarily oxygen based, and at the BZ center, it is described by polarization vectors as shown on Fig. 1. We see that our theory correctly predicts a softening of this mode as it approaches the zone boundary

TABLE I. Calculated phonon frequencies (in THz) and Grüneisen constants at Γ and X points of the Brillouin zone, the phonon group velocities ($\times 10^2$ m/s) estimated along (001) direction as well as contributions to lattice thermal conductivity ($W\,m^{-1}\,K^{-1}$) at $T = 1000$ K for UO_2 and PuO_2.

			UO_2			
Branch	$\omega(\Gamma)$	$\gamma(\Gamma)$	$\omega(X)$	$\gamma(X)$	v_g	κ
TA	0.00	0.00	3.88	−1.41	6.76	0.08
LA	0.00	0.00	6.45	−0.50	11.23	1.68
TO1	9.70	−1.32	9.38	−0.15	−0.55	∼0
LO1	13.51	0.43	8.03	−2.17	−9.53	0.11
TO2	14.22	−0.20	14.42	−0.62	0.31	∼0
LO2	16.14	0.62	17.81	−0.45	2.95	∼0
			PuO_2			
Branch	$\omega(\Gamma)$	$\gamma(\Gamma)$	$\omega(X)$	$\gamma(X)$	v_g	κ
TA	0.00	0.00	3.89	−1.59	6.67	0.08
LA	0.00	0.00	6.68	−0.54	11.48	1.50
TO1	10.21	−1.75	11.27	−0.43	1.84	∼0
LO1	15.03	0.27	8.56	−2.49	−11.10	0.16
TO2	16.07	−0.52	15.42	−0.95	−1.02	∼0
LO2	17.15	0.54	18.43	−0.60	2.46	∼0

X point although it underestimates the experimental value of the frequency by a factor of 2 for UO_2 and, most likely, also for PuO_2. Note that similar discrepancies have been detected by us earlier in studying lattice vibrations of Plutonium metal [22,23]. It is interesting to note that the same type of behavior for optical modes can be found in other materials with similar crystal structures, such as CaF_2 [25]. Since, the phonon dispersions in these systems can be well fit by utilizing the shell model where various structural sums entering the calculation are ultimately able to capture this behavior, it must be the peculiarity of the fluorite structure that dictates the dispersion of the mode LO1, and not other effects, such, e.g., as a dynamic Jahn-Teller interaction.

As we have gained access to the phonon dispersions, we are ready to discuss the lattice thermal conductivity in these systems which can be expressed for a cubic solid via the phonon frequencies $\omega_{\mathbf{q}j}$, group velocities $v_{\mathbf{q}j}$, phonon mean free paths $l_{\mathbf{q}j}$, and the Bose–Einstein distribution functions $N_{\mathbf{q}j}$ as follows [1]:

$$\kappa = \sum_{\mathbf{q},j} \omega_{\mathbf{q}j} v_{\mathbf{q}j} l_{\mathbf{q}j} \frac{\partial N_{\mathbf{q}j}}{\partial T}. \quad (1)$$

It is generally known that various scattering processes determine the temperature dependent phonon mean free paths. These, for example, include normal phonon-phonon interactions where one phonon with wave vector q gets scattered with the creation of two phonons with wave vectors $\mathbf{q}_1$ and $\mathbf{q}_2$ such that $\mathbf{q} = \mathbf{q}_1 + \mathbf{q}_2$, and umklapp phonon scattering processes where the quasimomentum conservation involves reciprocal lattice vector $\mathbf{G}$ such that $\mathbf{q} = \mathbf{q}_1 + \mathbf{q}_2 + \mathbf{G}$. At high temperatures which we are interested in, only umklapp processes are significant [1], and the phonon mean free paths can be evaluated from the knowledge of the third-order anharmonicity coefficients, which can be approximated by the dimensionless Grüneisen constants describing the change in the phonon frequency with respect to the atomic volume, i.e., $\gamma_{\mathbf{q}j} = d\ln\omega_{\mathbf{q}j}/d\ln V$. Hence, the efficiency of each phonon mode in the heat conduction is directly related to its group velocity but inversely proportional to the square of its Grüneisen constant [1].

Looking at the phonon spectra presented in Fig. 2 and 3, it is now clear that the best heat carriers are either the acoustic branches or the longitudinal optical branch LO1 which, in fact, has anomalously large group velocity along (001) (experimentally, its $v_{\mathbf{q}j}$ is twice the LA branch). One may then question why UO_2 or PuO_2 are known to be such inefficient thermal conductors. When compared to most semiconducting solids where optical modes exhibit rather weak wave vector dispersions and thus do not participate in the heat transfer, here the situation is much more favorable. The answer lies in the anomalously large anharmonicity associated with the LO1 mode, making its mean free path significantly shorter.

To make a comparative analysis, we have calculated the Grüneisen constants $\gamma_{\mathbf{q}j}$ associated with each vibrational mode at the Γ and X points of the Brillouin Zone. The results of these calculations are summarized in Table I. As one can see, the transverse acoustic modes have relatively large anharmonicity characterized by $\gamma = -1.41$ and $\gamma = -1.59$ for UO_2 and PuO_2, respectively. These values remarkably decrease for the LA modes ($\gamma = -0.50$ and -0.54) which at the same time show large group velocity. However, they become huge for the most dispersive LO1 mode. Here, the frequency at Γ shows positive γ (equal to 0.43 and 0.27) meaning that it decreases upon compression while the frequency at X shows negative γ (equal to -2.17 and -2.49) meaning its increase upon compression. Effectively, these two effects will add up to each other and result in the effective Grüneisen constants equal to -2.60 for UO_2 and -2.76 for PuO_2.

With these data in hand, we are able to estimate contributions to the lattice thermal conductivity κ from various phonon modes. Using a simple Debye-like linear approximation for the phonon dispersion and including corrections found empirically for the optical branches [26], the results of such estimates at a temperature $T = 1000$ K are presented in the last column of Table I. We can conclude that the only efficient heat carriers in both nuclear materials are their longitudinal acoustic phonons. The TA modes have relatively small contribution because of their smaller group velocities and relatively large γ, while the LO1 modes also do not much contribute due to their huge Grüneisen constants which completely compensate the effect of their largest $v_{\mathbf{q}j}$. The other modes have a negligible influence on κ.

The total value of κ in our calculation is a factor of 2 lower than the experimentally known thermal conductivity of UO_2 equal to 3.9 $W\,m^{-1}\,K^{-1}$ at $T = 1000$ K [27]. This is naturally connected to the approximate character of treating anharmonic effects. However, we believe that the relative contributions from various branches are captured correctly in our estimates, which gives a fundamentally new insight into the processes and factors that control thermal conductivity in these materials. As a result, we finally discuss the origins of the large anharmonicity of the most intriguing longitudinal optical mode LO1. As shown on Fig. 1, this mode is primarily oxygen driven. Oxygens are arranged in a cubic lattice with uranium or plutonium atoms occupying every other center of the cube. It is then clear that the structure is far from close packing, and the displacements of oxygens would involve the third-order anharmonic effects. Namely, they were used to explain the Debye-Waller factors in UO_2 many years ago [28]. To reduce anharmonicity, one may think of mixing these materials with elements filling in the cubic interstitials of the lattice and preventing large ionic excursions. One example could be oxygen overdoped materials UO_{2+x} and PuO_{2+x} where the latter one has been recently studied theoretically [7,8], but in view of enormous past experimental work on UO_{2+x}, consideration of dopants other than oxygen may be needed.

To summarize, using the LDA + DMFT method and linear response theory, we have studied lattice dynamical properties of UO_2 and PuO_2. Contributions to lattice thermal conductivity from various phonon modes were uncovered using the calculated group velocities and the Grüneisen constants. It was found that the dispersive longitudinal optical modes do not participate much in the heat transfer due to their large anharmonicity. Material design of systems with the last effect suppressed would open new possibilities to build more efficient fuels for modern nuclear industries. It is interesting to mention at the end that similar effects are expected in other materials with fluorite structure.

The authors are indebted to M. J. Gillan, G. Kotliar, and J. Thompson for useful conversations. The work was supported by the NSF Grants Nos. 0608283, 0606498 and by the US DOE Grant No. DE-FG52-06NA2621.

[1] *Thermal Conductivity: Theory, Properties, and Applications*, edited by Terry M. Tritt (Kluwer Academic, New York, 2004).
[2] P. J. D. Lindan *et al.*, J. Phys. Condens. Matter **3**, 3929 (1991).
[3] S. Motoyama *et al.*, Phys. Rev. B **60**, 292 (1999).
[4] S. Y. Savrasov *et al.*, Nature (London) **410**, 793 (2001).
[5] G. Lander, Science **301**, 1057 (2003).
[6] J. H. Shim *et al.*, Nature (London) **446**, 513 (2007).
[7] L. Petit *et al.*, Science **301**, 498 (2003).
[8] P. A. Korzhavyi *et al.*, Nat. Mater. **3**, 225 (2004).
[9] X. Wu *et al.*, Eur. Phys. J. B **19**, 345 (2001).
[10] I. D. Prodan *et al.*, J. Chem. Phys. **123**, 014703 (2005).
[11] I. D. Prodan *et al.*, Phys. Rev. B **73**, 045104 (2006); I. D. Prodan *et al.*, *ibid.* **76**, 033101 (2007).
[12] K. Kudin *et al.*, Phys. Rev. Lett. **89**, 266402 (2002).
[13] M. Colarieti-Tosti *et al.*, Phys. Rev. B **65**, 195102 (2002).
[14] *Theory of Inhomogeneous Electron Gas*, edited by S. Lundqvist and S. H. March (Plenum, New York, 1983).
[15] G. Kotliar *et al.*, Rev. Mod. Phys. **78**, 865 (2006).
[16] A. Georges *et al.*, Rev. Mod. Phys. **68**, 13 (1996).
[17] G. Kotliar *et al.*, Phys. Today **57**, No. 3, 53 (2004).
[18] J. Schoenes, Phys. Rep. **63**, 301 (1980).
[19] S. Y. Savrasov *et al.*, Phys. Rev. Lett. **96**, 036404 (2006).
[20] T. Miyake *et al.*, Phys. Rev. B **77**, 085122 (2008).
[21] S. Y. Savrasov *et al.*, Phys. Rev. Lett. **90**, 056401 (2003).
[22] X. Dai *et al.*, Science **300**, 953 (2003).
[23] J. Wong *et al.*, Science **301**, 1078 (2003).
[24] G. Dolling *et al.*, Can. J. Phys. **43**, 1397 (1965).
[25] M. M. Elcombe *et al.*, J. Phys. C **3**, 492 (1970).
[26] P. G. Klemens, Phys. Rev. **148**, 845 (1966).
[27] R. Brandt *et al.*, J. Non-Equilib. Thermodyn. **1**, 3 (1967).
[28] K. D. Rouse *et al.*, Acta Crystallogr. Sect. B **24**, 117 (1968).